

Long-range surface plasmon polariton nanowire waveguides for device applications

K. Leosson,¹ T. Nikolajsen,² A. Boltasseva³ and S. I. Bozhevolnyi⁴

¹Science Institute, University of Iceland, Dunhagi 3, IS-107 Reykjavik, Iceland

²Crystal Fibre A/S, Blokken 84, DK-3460 Birkerød, Denmark

³COM•DTU, Ørsted's Plads, Bldg. 345v, DK-2800 Kgs. Lyngby, Denmark

⁴Department of Physics and Nanotechnology, Aalborg University, Pontoppidanstræde 103, DK-9220 Aalborg Øst, Denmark

k.leosson@raunvis.hi.is

Abstract: We report an experimental study of long-range surface plasmon polaritons propagating along metallic wires of sub-micrometer rectangular cross-sections (nanowires) embedded in a dielectric. At telecom wavelengths, optical signals are shown to propagate up to several millimeters along such nanowires. As the wires approach a square cross-section, the guided mode becomes more symmetric and can, for example, be tuned to match closely the mode of a standard single-mode optical fiber. Furthermore, symmetric nanowires are shown to guide both TM and TE polarizations. In order to illustrate the applicability of plasmonic nanowire waveguides to optical circuits, we demonstrate a compact variable optical attenuator consisting of a single nanowire that simultaneously carries light and electrical current.

©2006 Optical Society of America

OCIS codes: (130.2790) Guided waves; (230.3120) Integrated optics devices; (230.7390) Waveguides, planar; (240.6680) Surface plasmons

References and Links

1. J. R. Krenn, H. Ditlbacher, G. Schider, A. Hohenau, A. Leitner, and F. R. Aussenegg, "Surface plasmon micro- and nano-optics," *J. Microscopy* **209**, 167-172 (2002).
2. W.L. Barnes, "Electromagnetic Crystals for Surface Plasmon Polaritons and the Extraction of Light from Emissive Devices," *J. Lightwave Technol.* **17**, 2170-2182 (1999).
3. J. Homola, S.S. Yee, and G. Gauglitz, "Surface plasmon resonance sensors: review," *Sensors Actuat. B* **54**, 3-15 (1999).
4. W.L. Barnes, A. Dereux, and T.W. Ebbesen, "Surface plasmon subwavelength optics," *Nature* **424**, 824-830 (2003).
5. J. J. Burke, G. I. Stegeman, and T. Tamir, "Surface-polariton-like waves guided by thin, lossy metal films," *Phys. Rev. B* **33**, 5186-5201 (1986).
6. P. Berini, *Opt. Lett.* **24**, 1011-1013 (1999); P. Berini, *Phys. Rev. B* **61**, 10484-10503 (2000).
7. R. Charbonneau, P. Berini, E. Berolo, and E. Lisicka-Shrzek, "Experimental observation of plasmon-polariton waves supported by a thin metal film of finite width," *Opt. Lett.* **25**, 844-846 (2000).
8. T. Nikolajsen, K. Leosson, and S. I. Bozhevolnyi, "In-line extinction modulator based on long-range surface plasmon polaritons," *Opt. Commun.* **244**, 455-459 (2005).
9. S.I. Bozhevolnyi, T. Nikolajsen, and K. Leosson, "Integrated power monitor for long-range surface plasmon polaritons," *Opt. Commun.* **255**, 51-56 (2005).
10. R. Charbonneau, N. Lahoud, G. Mattiussi, and P. Berini, "Demonstration of integrated optics elements based on long-ranging surface plasmon polaritons," *Opt. Express* **13**, 977-984 (2005).
11. A. Boltasseva, T. Nikolajsen, K. Leosson, K. Kjær, M. L. Larsen, and S. I. Bozhevolnyi, "Integrated Optical Components Utilizing Long-Range Surface Plasmon Polaritons," *IEEE J. Lightwave Technol.* **23**, 413-422 (2005).
12. P. Berini, "Optical Waveguide Structures," US patent number 6,741,782 (<http://www.uspto.gov/>).
13. T. Mizuno, H. Takahashi, T. Kitoh, M. Oguma, T. Kominato, and T. Shibata, "Mach-Zehnder interferometer switch with a high extinction ratio over a wide wavelength range," *Opt. Lett.* **30**, 251-253 (2005).

1. Introduction

Optics of surface plasmon polaritons (SPPs) and, in particular, of plasmonic nanostructures, currently attracts considerable interest. Plasmon propagation and scattering in metallic nanostructures has been studied experimentally and theoretically (see, e.g., Ref. [1] and references therein) and a number of optical devices incorporating SPPs have been proposed, such as light-emitting diodes with improved extraction efficiency [2], sensors [3], or novel devices for routing and controlling light signals on a sub-wavelength scale [4]. A serious limitation to the applicability of SPP devices for optical signal processing, however, is the high propagation loss associated with SPPs at optical frequencies, the difficulty of efficiently coupling light in and out of the structure and the fact that only TM polarized light propagates along the metal-dielectric interface.

Another avenue of SPP research focuses on so-called long-range surface plasmon polaritons (LRSPPs) propagating on nanometer-thin metal films or stripes embedded in a dielectric material [5-7]. In essence, an LRSPP represents a coupled mode involving two SPP waves propagating on the upper and lower surface of the metal film. For sufficiently thin metal films, the propagation loss of LRSPPs is significantly reduced compared to uncoupled SPP waves and, furthermore, LRSPPs in metal stripe waveguides can be directly excited using standard optical fibers with low coupling loss using the end-fire method [7]. LRSPP waveguides based on thin metal stripes have been used to realize a range of integrated optical devices [8-11] but these still suffer the limitation of only allowing propagation of TM polarized light.

In the present work, we report measurements on LRSPP waveguides that consist of metallic wires with sub-micrometer dimensions in width and thickness (nanowires) embedded in a homogeneous dielectric. Such nanowire waveguides have previously been proposed and analyzed theoretically [12] but to our knowledge no experimental studies of such structures exist in the literature. Waveguides with a symmetric (square) cross section are of particular interest since they are expected to guide both TE and TM polarized light. If acceptable propagation and coupling losses can be realized, such waveguides can provide an electrically conductive alternative to conventional dielectric waveguides in optical devices.

2. Experiment

The nanowires were fabricated as follows: A silicon wafer was coated with a 15- μm thick layer of BCB (Cyclotene 3022-57, DOW Chemical Company). A layer of ZEP520 electron-beam resist was spun on top of the BCB layer and stripes of different width were written using a JEOL JBX 9300FS electron-beam lithography system. Nanowires were fabricated by deposition of thermally evaporated gold layers (100, 150 and 200 nm) and a subsequent lift-off process. Continuous (electrically conducting) nanowires with aspect ratios (width to height) down to about unity could be fabricated in this fashion. The nanowires were covered by a second 15- μm layer of BCB. In order to make variable optical attenuators, nanowire waveguides were connected to contact pads, defined by optical lithography and deposited separately before applying the second layer of BCB. In this case, contact holes were made through the top cladding using an Al etch mask (patterned by photolithography and lift-off) followed by reactive ion etching. For cutback measurements, nanowire samples were cut to different lengths using a dicing saw.

Light at 1550 nm wavelength was launched from a tunable laser, through a polarization-maintaining fiber, and coupled directly to the metal nanowires through the sample facet (end-fire coupling). The output from the nanowire was imaged through a polarizer onto a vidicon camera for mode field measurements. The polarization of the in-coupling fiber was tilted 45 degrees with respect to the waveguide axes. The waveguide output was measured separately for TM and TE polarizations using a polarizing filter, without changing the alignment of the input fiber. Insertion loss measurements were made by coupling TM polarized light into the waveguides, picking up the output with a standard single-mode fiber and measuring with a photodetector. Sample facets were not polished after dicing but index-matching liquid was used between fiber and sample to improve the coupling conditions.

3. Results

Figure 1 shows the output from three 2-mm long nanowire waveguides of 150-nm thickness and different width. The approximate aspect ratio is indicated by the white rectangles in the lower set of figures. Horizontal and vertical mode profiles for the three waveguides are plotted in Fig. 2. In all cases where the width of the waveguide is greater than the height, only TM polarized light is observed at the output. The narrowest waveguide, on the other hand, where the cross section is close to square shape, clearly guides both TM and TE polarized light.

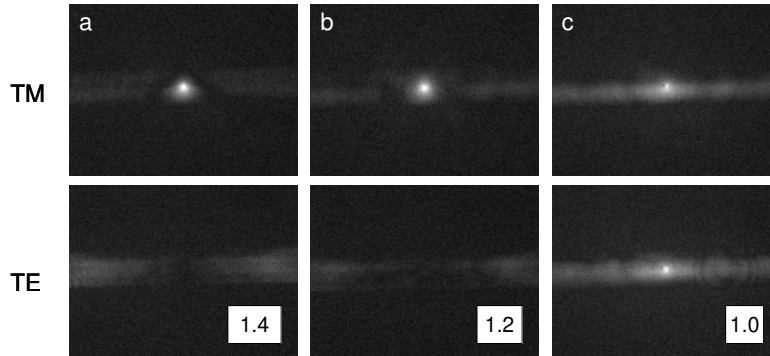


Fig. 1. Output facets of nanowire waveguides having different width-to-height aspect ratios. Polarized light is launched into the waveguides with a polarization direction rotated 45° with respect to the TE/TM axes of the waveguides.

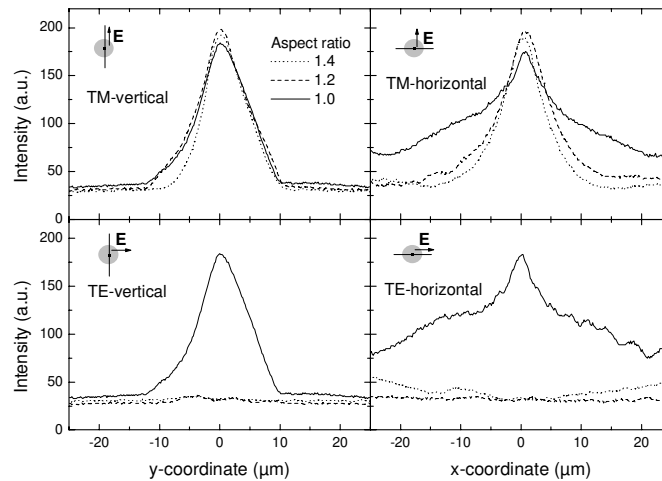


Fig. 2. Vertical (left column) and horizontal (right column) mode profiles for TM (top row) and TE (bottom row) polarizations, derived from the images in Fig. 1. For asymmetric waveguides only one polarization is guided while for the symmetric case (aspect ratio close to 1) both TE and TM-polarized modes are observed at the output.

The mode-field diameter (MFD) for the profiles shown in Fig. 2 are in the range 12-14 μm when approximated with a Gaussian function, increasing slightly as the waveguide becomes narrower, consistent with weaker confinement. The TE and TM modes in the narrowest waveguide are similar as expected from a symmetric core shape. The difference in the vertical

and horizontal profiles arises from the finite width of the cladding in the vertical direction. A sudden increase in scattered light in the cladding layers is also evident in the case of the narrowest waveguide. This sudden increase cannot be explained simply by increase in coupling loss and is most likely due to limitations of the fabrication process. Generally, it was observed that waveguides with aspect ratio close to unity had an increasing number of defects (discontinuities) and exposed waveguides with widths smaller than the deposited thickness did not survive the lift-off process. This issue can most likely be solved through optimization of the lithographic process, better metal deposition techniques, etc.

Propagation loss and coupling loss for TM-polarized light propagating in nanowire waveguides of different width was estimated using the standard cut-back method. Results are plotted in Fig. 3. As expected, the propagation loss is higher for wider waveguides, due to increased absorption (Ohmic loss). For the narrowest wires, a propagation loss of about 0.5 dB/mm is observed, corresponding to a propagation length ($1/e$) of nearly 8 mm. This is similar to the smallest propagation loss reported for thin LRSPP stripe waveguides embedded in BCB [11]. However, since the loss for the narrowest waveguides is influenced by scattering out of the waveguide well as loss in the BCB cladding, we believe that considerably lower propagation loss values can be realized by improving the structural quality of the waveguides and by selecting cladding materials with a higher internal transmission in the telecom wavelength range. Ref. [12] predicts a propagation loss of 0.1 dB/cm for 150-nm square Au waveguides in SiO₂ while the propagation and coupling losses for the narrowest waveguides in Fig. 3 agree with the calculated values for a 170-nm square waveguide.

The propagation loss of TE-polarized light in the symmetric waveguides was similar to that of TM-polarized light. However, due to the large relative uncertainty of the propagation loss values we were not able to determine the polarization dependent loss (PDL) for these waveguides. It is clear from Fig. 3 that in order to simultaneously minimize propagation loss in nanowire waveguides and coupling loss to a standard single-mode fiber, some form of mode conversion is required. There will also be a tradeoff between bend loss and propagation loss and therefore the optimum waveguide dimensions will depend on the device geometry in each particular case.

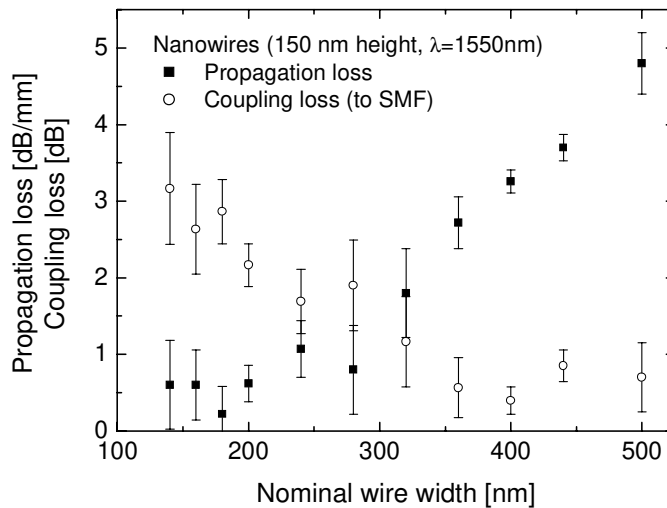


Fig. 3. Propagation loss and coupling loss in nanowire waveguides of different dimensions, derived from a cut-back measurements. Reducing the wire dimensions increases the mode size and reduces the Ohmic loss due to a smaller field-metal overlap.

4. Variable optical attenuator

LRSPP nanowire waveguides do not provide a route to large-scale integration of optical circuits since the light field associated with these waveguides is still comparable to standard low-

index-contrast dielectric waveguides. However, the nature of LRSPP waveguides introduces new design possibilities for optical devices that are compatible with the current standard technology platform and can result in smaller device footprint and/or improved performance. Nanowires can, for example, be used simultaneously as waveguides and heating elements in thermo-optic devices. Such devices rely on a temperature-induced change in the refractive index of the material in the region of the mode field. In conventional thermo-optic devices, the placement of heating elements introduces a trade-off between light absorption by electrodes and heating efficiency and uniformity. Current passed through a nanowire efficiently heats the immediate vicinity of the waveguide, resulting in an improved power budget, faster response times, and offers the possibility of individually heating closely spaced waveguides.

As an example of a simple functional circuit based on plasmon waveguiding in nanowires, we fabricated variable optical attenuators based on 1.6-mm long straight nanowire waveguides with electrical contacts at each end. Similar devices have been fabricated previously using thin stripe waveguides [8]. The length of the heated section was 1 mm. The insertion loss (fiber-to-fiber) of devices having different wire widths is shown in Fig. 4, together with a schematic picture of the device. The measurements were made using TM-polarized light at 1550 nm wavelength. The electrical resistance of the waveguides investigated here was around 500-800 Ω , as shown in the inset, but increased rapidly as the wire dimensions approached a square cross section. We did not succeed in realizing electrically conductive TE-guiding devices due to problems in our current fabrication process, as described above.

The different devices exhibit similar performance when the response is plotted as a function of drive power. The effect of stronger confinement by wider waveguides can be seen as a flat plateau in the response curve at low drive power. The shoulder at 20-25 mW drive power presumably relates to internal reflections in the device.

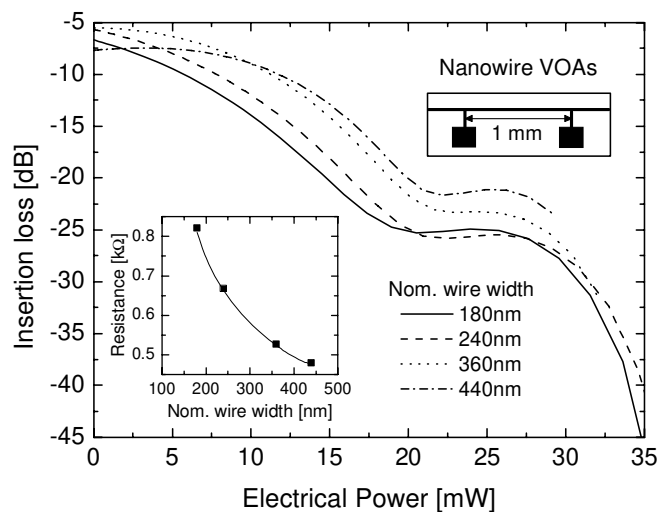


Fig. 4. Response curves for optical attenuators based on LRSPP nanowire waveguides. Electrical current passes through the waveguide core between the contact pads and results in local heating of the waveguide, gradually reducing its effective index. The inset shows the electrical resistance of the investigated devices.

The maximum drive voltage used for the devices tested here was in the range 4-5V. With these voltages it is possible to reach extinction ratios in excess of 40 dB which is comparable to the extinction ratio achieved in state-of-the-art optical attenuators based on planar light-wave circuits (PLCs) [13]. The LRSPP nanowire attenuator operates by reducing index guiding rather than by interference and therefore shows less pronounced wavelength dependence than conventional Mach-Zehnder type attenuators and has a considerably smaller footprint.

Finally, with improved process control and device design, it should be possible to fabricate LRSPP devices with low insertion loss that support both polarizations and exhibit a low polarization-dependent loss, even at high extinction ratios.

5. Conclusions

We have demonstrated guiding of long-range surface plasmon polaritons along metallic nanowires at 1550 nm and the advantage of using nanowire waveguides in specific types of integrated optical devices. The electrical conductivity of the waveguides opens new design possibilities, e.g. for thermo-optical components, using a device platform which is compatible with standard optical fibers and low-index-contrast dielectric PLCs.